EFFICIENCY OF CAPACITOR IN CCTO CERAMICS WITH ACTIVATED CARBON DERIVED FROM TAMARIND FRUIT SHELLS

Sanit Suwanwong* and Artit Hutem

Physics Division, Faculty of Science and Technology, Phetchabun Rajabhat University

*corresponding author e-mail: sanit.suw@gmail.com

(Received: 20 January 2021; Revised: 10 April 2021; Accepted: 20 April 2021)

Abstract

Sweet tamarind is one of the important economic corps which tamarind fruit shells go to waste after being removed. In this study, tamarind fruit shells activated using KOH and rinsed with HCl under ambient pressure were used to synthesize activated carbon with high carbon porosity. After that, $CaCu_3Ti_4O_{12}$ (CCTO) with high dielectric constant was synthesized using simplified method and added activated carbon in the proportion of 10, 15, 25 and 50 mol%, respectively. The results from XRD analysis of carbon phases and SEM analysis of particle profile and porosity showed that at 50 mol% phase of carbon increases and high porosity was found. Additionally, the activated carbon derived from tamarind fruit shells with 50 mol% was studied for its efficiency of capacitance, dielectric constant and dielectric loss using Impedance analyzer. It was found that CCTO with activated carbon derived from tamarind fruit shells at 50 mol% had the highest electrical capacitance and dielectric constant at 50 Hz accounting for 63-time higher than that of CCTO without activated carbon derived from tamarind fruit shells. The results also suggested that the capacitance, dielectric constant and dielectric loss decreased when the frequency was higher. This means that activated carbon derived from tamarind fruit shells increases the capacitance of CCTO ceramics and makes it suitable for the invention of electrical capacitors.

Keywords: Capacitor, Dielectric, CCTO, Activated carbon, Tamarind fruit shells

INTRODUCTION

Sweet tamarind is one of the important economic corps which tamarind fruit shells go to waste after being removed. However, tamarind fruit shells can be synthesized to activated carbon with high porosity resulting in a large surface area (Sudhan et al., 2017). When it is added to some certain materials, activated carbon can enhance the efficiency of energy storage and electrical charges, become photocatalyst and improve electrical performance of a variety of electronic devices such as resistor, transistor and capacitor.

Capacitors are electrical energy storage devices. They are available on the market in a wide range of formats such as mica capacitor, plastic film capacitor, electrolytic capacitor, tantalum capacitor and ceramic capacitors. Ceramic capacitor is exceptionally durable. Apart from the ability to store electric charge, the ability to hold the charge should be under consideration with sintering at high temperature (Prasertpalichat et al, 2017). This can be verified from dielectric loss, that is, low dielectric loss represents the ability to hold more electric charge. Perovskite–like titanate compounds ($ATiO_3$) with the chemical formula AMO_3 is the most widely used material in ceramic capacitors. Its properties include semiconductor, catalyst, sensing, ferroelectric, ferromagnetic (Bhalla, Guo, & Roy, 2000; Jaiban et al., 2015) as well as illumination and capacitor application. It can also conduct electric when exposed to light such as strontium titanate $SrTiO_3$ (Suwanwong et al., 2015) and calcium copper titanate $CaCu_3Ti_4O_{12}$ (Lui et al., 2015). For $CaCu_3Ti_4O_{12}$ (CCTO) exhibits a giant dielectric constant value (Masingboon et al., 2013) by using internal–barrier–layer–capacitor model (Sinclair et al., 2002). It is suitable for the invention of ceramic capacitors used for electronic devices.

The aim of this study is to increase the efficiency of the CCTO capacitors by adding activated carbon derived from tamarind fruit shells. The pellets of CCTO through a sintering process to form ceramic properties which give high electric charge were used to enhance dielectric properties and efficiency of CCTO ceramic capacitor by adding activated carbon derived from tamarind fruit shells. To be able to invention of capacitors used for electronic devices with high capacitance.

MATERIALS AND METHODS

1. Preparation of activated carbon from tamarind fruit shells

To obtain activated carbon from tamarind pods in this study, tamarind fruit shells were rinsed with distilled water and dried at 80°C for 24 h before they were ground and carbonized. In the stage of carbonization, 400 grams of dried ground tamarind fruit shells were calcinated at 400°C for 1 h (5°C increased every minute) under ambient pressure. Through the aforementioned pre–activation process, 16.8 grams of before activation tamarind fruit shells carbon (BA–TPC) were produced. After that, the researchers mixed 3 M concentration of potassium hydroxide (KOH) with 40 grams DI water, and slowly added 45 grams of the mixture to BA–TPC to a ratio of 1 : 3 by weight afterwards. This compound was left for 3 h before it was calcinated at 400°C for 1 h under ambient pressure to produce tamarind fruit shells activated by KOH (TPC–KOH). The TPC–KOH, then, was flushed with DI water and 1 M hydrochloric acid (HCl) back and forth until pH7 was reached. Next, the compound was dried at 80°C for 5 h. This process yielded porous carbon which, after activation, became AA–TPC or activated carbon derived from tamarind fruit shells.

2. Production of powered CCTO

In the production of powered CCTO, stoichiometry according to the chemical equation 1 was used for quantitative calculation of materials required.

$$CaCO_3 + 3CuO + 4TiO_2 \longrightarrow CaCu_3Ti_4O_{12} + CO_2 \quad (1)$$

In this study, the mole ratio was 1 mole $CaCO_3$ (Sigma–Aldrich), 3 moles CuO and 4 moles TiO_2 (Sigma–Aldrich). The materials were milled for 2 h and calcined at 600°C for 12 h to produce calcined CCTO which, then, was sifted using a 120–mesh sieve. After that, the researchers added two drops of polyvinyl alcohol (PVA) (Sigma–Aldrich) mixed with 5% of water into the calcined CCTO and sifted again using a 40–mesh sieve. Subsequently, the mixture of CCTO and PVA was put into a 1.5 cm cylindrical–shape mold and pellet using 0.5 tons pressure before sintering 1,000°C for 8 h. Through the aforementioned steps, ceramic CCTO without activated carbon derived from tamarind fruit shells was obtained. In order to gain CCTO with activated carbon derived from tamarind fruit shells, the calcined CCTO was mixed with 10, 15, 25 and 50 mol% of activated carbon derived from tamarind fruit shells using sonicator for 1 h under the process mentioned earlier.

3. Investigation of phase patterns using X–ray diffraction technique

The investigation of phase patterns of activated carbon derived from tamarind fruit shells, CCTO and CCTO with activated carbon derived from tamarind fruit shells was conducted in 2–theta range of 20–80° using X–ray diffraction (XRD) technique (Bruker, model D2 PHASER, Germany).

4. images of activated carbon and CCTO with activated carbon derived from tamarind fruit shells using Scanning Electron Microscope

The analysis showed the images of activated carbon derived from tamarind fruit shells, CCTO and CCTO with activated carbon derived from tamarind fruit shells formed through Scanning Electron Microscope (SEM) (JEOL, model JSM–6010LV, Japan). This allowed the researchers to see particle images of activated carbon derived from tamarind fruit shells, CCTO and CCTO with activated carbon derived from tamarind fruit shells.

5. Dielectric constant and dielectric loss measurement

For the measurement of capacitance of CCTO ceramics, electrodes had been made on both sides of CCTO ceramic pellets using conductive silver paint of SPI Supplies Division of STRUCTURE PROBE, Inc. before CCTO and CCTO with activated carbon derived from tamarind fruit shells were placed between two copper plates and connected to the electrodes. Then, impedance analyzer (HIOKI, model IM 3570, Japan) at a frequency of 50 Hz – 1 MHz was connected to electrodes to measure capacitance (C) and dielectric loss of CCTO and CCTO with activated carbon derived from tamarind fruit shells. The capacitance (C) used to calculate dielectric constant (ε_r) was shown in equation 2.

$$C = \frac{\varepsilon_r \varepsilon_0 A}{d} \quad (2)$$

Where C is capacitance (Farad).

ε_r is dielectric constant.

ε_0 is vacuum permittivity (ε_0 = 8.85 x 10^{-12} F/m).

A is surface area (m^2).

d is thickness (m).

RESULTS

1. Phase patterns of activated carbon and CCTO with activated carbon derived from tamarind fruit shells using X–ray diffraction technique

At the initial step of synthesis, activated carbon derived from tamarind fruit shells called BA–TPC was produced. It was a pre–activation process which involved carbonization of tamarind fruit shells with ambient pressure. Then, the activation was performed with a base, KOH. The sample made at this stage was called TPC–KOH. The last step was rinsing the substance with distilled water (DI) and HCl acid until pH7 was reached and dried it. This process yielded porous carbon which is activated carbon derived from tamarind fruit shells (Senthilkumar et al., 2013) called AA–TPC. Phase of the three samples of activated carbon derived from tamarind fruit shells were analyzed using X–ray diffraction (XRD) as shown in Figure 1. The results from 2–theta range of 20–80° showed that BA–TPC consisted of C8 carbon (ICSD code: 020351) with (110) and (203) planes, Graphite (ICSD code: 088811) with (110) and (022) planes and Diamond (ICSD code: 088818) with (200), (112) and (220) planes. It was found that the peaks of all phases of BA–TPC decreased when BA–TPC was activated by KOH. However, when making the sample a base using DI and HCl, the results showed that the peaks of all phases of AA–TPC, as a yield of the process, was identical with BA–TPC but its peaks of all phases were a bit higher. Therefore, after the sample was activated and reached pH7, the properties of carbon were higher.

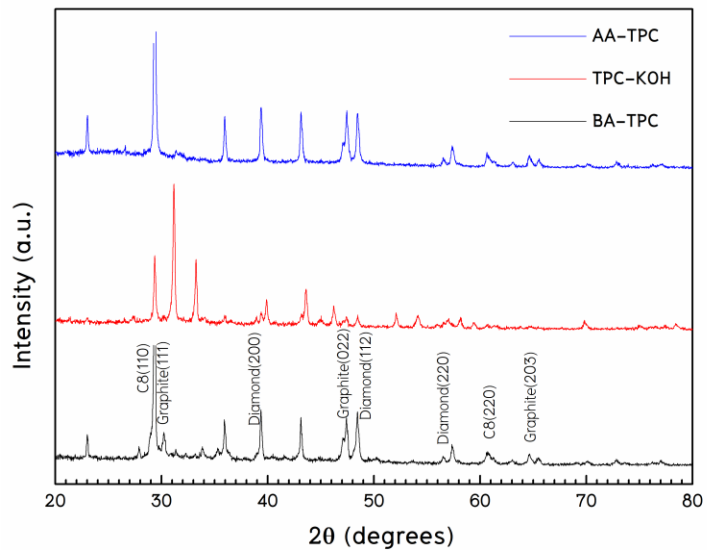

Figure 1 Phase patterns of activated carbon derived from tamarind fruit shells.

To synthesize Perovskite–like (CCTO_STD), CCTO, activated carbon derived from tamarind fruit shells was added into CCTO in the proportion of 10, 15, 25 and 50 mol% (CCTO_AA), respectively and sintering process at 1000 °C for 8 h was performed. The phase patterns were analyzed using X–ray diffraction (XRD) as shown in Figure 2. The results showed that the samples consisted of CCTO ceramic structure (ICSD code: 030592) with (220), (310), (400) and (440) planes together with C structure with (220) plane and C8 structure with (220) plane. Additionally, the highest increase of C and C8 which occurred when adding CCTO with 50 mol% (CCTO_AA50) offered higher carbon and the highest plane of CCTO at (440).

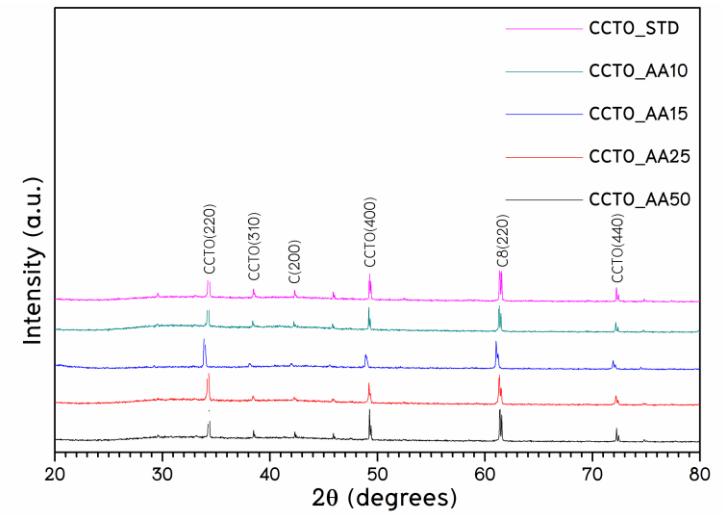

Figure 2 Phase patterns of CCTO with activated carbon derived from tamarind fruit shells.

2. SEM images of activated carbon and CCTO with activated carbon derived from tamarind fruit shells

SEM images in Figure 3 showed as follows: a) calcined BA–TPC before activation, b) TPC–KOH with KOH activation to which KOH is attached and C) AA–TPC or activated carbon derived from tamarind fruit shells as a result of pH7 from DI water and HCl acid which porosity of carbon was higher than that of BA–TPC.

SEM images in Figure 4 showed particles of samples sintered at 1000°C for 8 h. It is apparent that the average particle size of CCTO (CCTO_STD) as shown in a) was the smallest compared with the other images which activated carbon derived from tamarind fruit

shells at 10, 15, 25 and 50 mol% were added in b) – e), respectively. The results suggested that the average particle size increases with the higher proportion of activated carbon derived from tamarind fruit shells. This is one of the reasons why a high dielectric constant was detected.

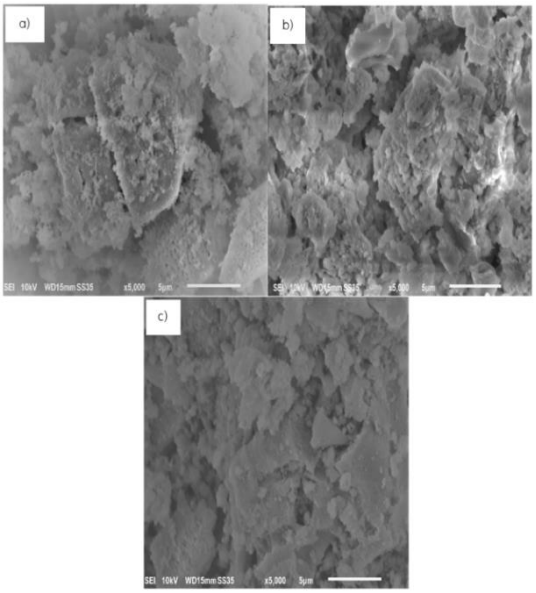

Figure 3 SEM images of activated carbon derived from tamarind fruit shells: a) BA–TPC, b) TPC–KOH and c) AA–TPC.

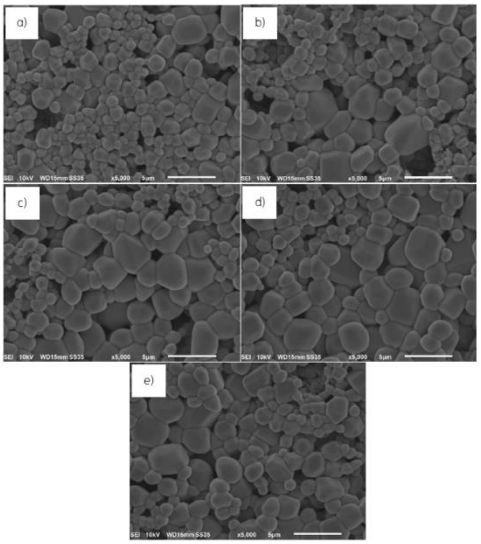

Figure 4 SEM images of CCTO: a) CCTO_STD, b) CCTO_AA10, c) CCTO_AA15, d) CCTO_AA25 and e) CCTO_AA50.

3. Dielectric constant and Dielectric loss values of CCTO with activated carbon derived from tamarind fruit shells

After adding activated carbon derived from tamarind fruit shells at 0, 10, 15, 25 and 50 mol% into CCTO and sintering at 1000 °C for 8 h, capacitance (C) and dielectric loss frequency 50 Hz – 1 MHz were measured using Impedance analyzer. According to Table 1, capacitance of all samples decreased when frequency was higher. The capacitance of CCTO with 50 mol% (CCTO_AA50) was 10,521 pF at 50 Hz, due to high porosity of activated carbon, making it the highest among all samples. On the other hand, the capacitance decreased when the proportion of activated carbon derived from tamarind fruit shells decreased.

Table 1 Capacitance of CCTO with activated carbon from tamarind fruit shells.

Type	C (pF)					
	50 Hz	100 Hz	1 kHz	10 kHz	100 kHz	1 MHz
CCTO_STD	167	75	44	32	26	21
CCTO_AA10	4605	2535	494	160	80	53
CCTO_AA15	6870	3612	742	257	125	81
CCTO_AA25	8401	4858	1118	362	170	105
CCTO_AA50	10521	6138	1345	427	194	121

The capacitance (C) of CCTO with 0, 10, 15, 25 and 50 mol% of activated carbon derived from tamarind fruit shells was used to calculate dielectric constant (ε_r using equation $C = \frac{\varepsilon_r \varepsilon_0 A}{d}$ as shown in Table 2. The results between the dielectric constant and the frequency in Hz were graphed as shown in Figure 5. It was found that the dielectric constant of all samples decreased when the frequency increased. However, the dielectric constant of CCTO with 50 mol% (CCTO_AA50) was the highest at 6464 at frequency 50 Hz due to its higher porosity. The dielectric constant was lower when less amount of activated carbon derived from tamarind fruit shells was added. Regarding dielectric loss of CCTO without activated carbon derived from tamarind fruit shells, the maximum loss was at 50 HZ and lowered to 126 kHz, then increased with higher frequency as shown in Figure 6. Dielectric

loss of CCTO with activated carbon derived from tamarind fruit shells, the dielectric loss of all samples decreased when the frequency increased.

Table 2 Dielectric constant values of CCTO with activated carbon from tamarind fruit shells.

Type	ε_r					
	50 Hz	100 Hz	1 kHz	10 kHz	100 kHz	1 MHz
CCTO_STD	1007	632	167	121	98	79
CCTO_AA10	3285	1808	352	114	57	38
CCTO_AA15	5145	2705	556	192	94	61
CCTO_AA25	5843	3379	778	252	118	73
CCTO_AA50	6464	3771	826	262	119	74

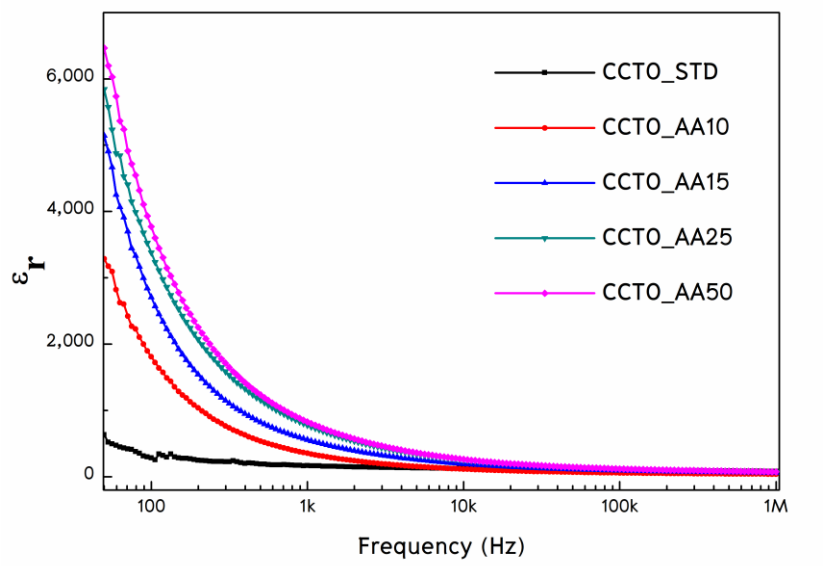

Figure 5 Dielectric constant values of CCTO with activated carbon derived from tamarind fruit shells.

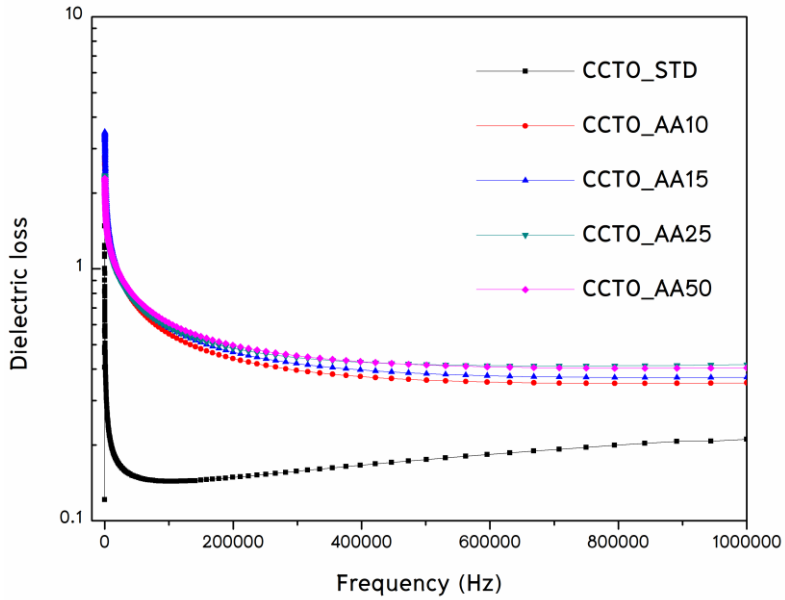

Figure 6 Dielectric loss of CCTO with activated carbon derived from tamarind fruit shells.

DISCUSSION

Phase pattern analysis of activated carbon derived from tamarind fruit shells using XRD technique showed that the peaks of all phrases were found in BA–TPC, TPC–KOH and AA–TPC; C8 with (110) and (203) planes, Graphite with (110) and (022) planes and Diamond with (200), (112) and (220) planes. The fact that the peaks of AA–TPC were slightly higher indicates that carbon increases after activation and pH7 value. The results showed CCTO (CCTO_STD) with 10, 15, 25 and 50 mol% of activated carbon derived from tamarind fruit shells had CCTO at (220), (310), (400) and (440) planes, respectively. Additionally, C with (220) plane, C8 with (220) plane and CCTO with 50 mol% of activated carbon increase the peaks and the highest phase of CCTO was at (440) plane. The analysis of SEM particles showed that the porosity of activated carbon derived from tamarind fruit shells (AA–TPC) which was activated and reached pH7 was the highest compared with inactivated BA–TPC.

The measurement of capacitance and dielectric constant of CCTO with and without activated carbon derived from tamarind fruit shells showed that CCTO with 50 mol% gave the greatest capacitance and dielectric constant at frequency 50 Hz accounting for 63 times of CCTO without activated carbon due to increased internal–barrier–layer–capacitor. The

higher activated carbon added, the higher porosity obtained (Senthilkumar et al., 2013), and this results in more efficient capacitance. Moreover, the capacitance and dielectric constant of all samples decreased with higher frequency. Dielectric loss of CCTO with activated carbon derived from tamarind fruit shells decreased if frequency increased. For CCTO without activated carbon, dielectric loss decreased with the increase of frequency at a certain point, but conversely increased when the frequency continued increasing.

When more activated carbon derived from tamarind fruit shells was added to CCTO, higher values of capacitance and dielectric constant were found. This indicates that the addition of activated carbon derived from tamarind fruit shells made CCTO ceramics more efficient in storing electric charges. Thus, it is suitable for the invention of capacitors used for electronic devices with high capacitance.

CONCLUSION

When the activated carbon derived from tamarind fruit shells (AA–TPC) reached pH7, its peaks of all phases were higher, indicating higher carbon and more porosity compared with BA–TPC without activation. The more activated carbon derived from tamarind fruit shells was added to CCTO, the higher carbon was detected. Additionally, CCTO at the plane of (440) was found the highest.

CCTO with 50 mol% of activated carbon offers the highest dielectric constant at frequency of 50 Hz accounting for 63 times higher than CCTO without activated carbon. This indicates that adding more activated carbon derived from tamarind fruit shells in CCTO capacitors resulted in the higher porosity obtained and higher dielectric constant due to increased internal–barrier–layer–capacitor. Moreover, the addition of activated carbon from tamarind fruit shells made CCTO ceramics more efficient in storing electric charges. Thus, it is suitable for the invention of capacitors used for electronic devices with high capacitance and electronics industry.

ACKNOWLEDGEMENT

This study was supported by Physics Division, Science Center, Faculty of Science and Technology and Research and Development Institute, Phetchabun Rajabhat University

which received funding from the annual government statement of expenditure for research and innovation projects to build fundamental knowledge in fiscal year 2019.

REFERENCES

Bhalla, A.S., Guo, R., & Roy, R. (2000). The Perovskite Structure – a Review of its Role in Ceramic Science and Technology. **Material Research Innovations, 4**(1), 3–26.

Jaiban, P., Suwanwong, S., Namsar, O., & Watcharapasorn, A. (2015). Simultaneous Tuning of the Dielectric Property and Photo– induced Conductivity in Ferroelectric $Ba_{0.7}Ca_{0.3}TiO_3$ via La doping. **Materials Letters, 147,** 29 – 33.

Lui, P., Lai, Y., Zeng, Y., Wu, S., Huang, Z., & Han, J. (2015). Influence of Sintering Conditions on Microstructure and Electrical Properties of $CaCu_3Ti_4O_{12}$ (CCTO) Ceramics. **Journal of Alloys and Compounds, 650,** 59 – 64.

Masingboon, C., Eknapakul, T., Suwanwong, S., Buaphet, P., Nakajima, H., Mo, S.–K., Thongbai, P., King, P.D.C., Maensili, S., & Meewasana, W. (2013). Anomalous Change in Dielectric Constant of $CaCu_3Ti_4O_{12}$ under Violet–to–Ultraviolet Irradiation. **Applied Physics Letters, 102,** 202903.

Prasertpalichat, S., Phutthichon, S., & Sumang, R. (2017). Effect of Sintering Temperature on Crystal Structure and Electrical Properties of BNT–BKT–BZT Lead–free Ceramic. **PSRU Journal of Science and Technology, 2(3),** 20–32.

Senthilkumar, S.T., Selvan, R.K., Melo, J.S., & Sanjeeviraja, C. (2013). High Performance Solid–State Electric Double Layer Capacitor from Redox Mediated Gel Polymer Electrolyte and Renewable Tamarind Fruit Shell Derived Porous Carbon. **ACS Applied Materials & Interfaces, 5,** 10541 – 10550.

Sinclair, D.C., Adams, T.B., Morrison, F.D. & West, A.R. (2002). $CaCu_3Ti_4O_{12}$: One–Step Internal Barrier Layer Capacitor. **Applied Physics Letters,** 80(12), 2153.

Sudhan, N., Subramani, K. Karnan, K., Ilayaraja, N., & Sathish, M. (2017). Biomass–Derived Activated Porous Carbon from Rice Straw for a High–Energy Symmetric Supercapacitor in Aqueous and Non–aqueous Electrolytes. **Energy Fuels, 31,** 977 – 985.

Suwanwong, S., Eknapakul, T., Rattanachai, Y., Masingboon, C., Rattanasuporn, S., Phatthanakun, R., Nakajima, H., King, P.D.C., Hodak, S.K., & Meewasana, W. (2015). The Dynamics of Ultraviolet–induced Oxygen Vacancy at the Surface of Insulating $SrTiO_3$ (001). **Applied Surface Science, 355,** 210 – 212.